

# Effect of Large Vehicles on Left Turn Gap Acceptance at Signalized Intersections



**SAFETY RESEARCH USING SIMULATION**

**UNIVERSITY TRANSPORTATION CENTER**

David A. Noyce, PhD

Professor

Department of Civil and Environmental  
Engineering

Boris Claros, PhD

Assistant Researcher

Department of Civil and Environmental Engineering  
University of Wisconsin – Madison

## Effect of Large Vehicles on Left Turn Gap Acceptance at Signalized Intersections

David A. Noyce, PhD  
Professor  
Department of Civil and Environmental  
Engineering  
University of Wisconsin – Madison  
<https://orcid.org/0000-0001-5887-8391>

Madhav Chitturi, PhD  
Assistant Research Scientist  
Department of Civil and Environmental  
Engineering  
University of Wisconsin – Madison  
<https://orcid.org/0000-0003-0580-3454>

Boris Claros, PhD  
Assistant Researcher  
Department of Civil and Environmental  
Engineering  
University of Wisconsin – Madison  
<https://orcid.org/0000-0002-4787-1749>

A Report on Research Sponsored by

SAFER-SIM University Transportation Center

Federal Grant No: 69A3551747131

May 2021

## **DISCLAIMER**

*The contents of this report reflect the views of the authors, who are responsible for the facts and the accuracy of the information presented herein. This document is disseminated in the interest of information exchange. The report is funded, partially or entirely, by a grant from the U.S. Department of Transportation's University Transportation Centers Program. However, the U.S. government assumes no liability for the contents or use thereof.*

## TECHNICAL REPORT DOCUMENTATION PAGE

<b>1. Report No.</b> UW-2-Y4	<b>2. Government Accession No.</b>	<b>3. Recipient's Catalog No.</b>	
<b>4. Title and Subtitle</b> Effect of Large Vehicles on Left Turn Gap Acceptance at Signalized Intersections		<b>5. Report Date</b> May 2021	
		<b>6. Performing Organization Code</b>	
<b>7. Author(s)</b> David A. Noyce, PhD <a href="https://orcid.org/0000-0001-5887-8391">https://orcid.org/0000-0001-5887-8391</a> Madhav Chitturi, PhD <a href="https://orcid.org/0000-0003-0580-3454">https://orcid.org/0000-0003-0580-3454</a> Boris Claros, PhD <a href="https://orcid.org/0000-0002-4787-1749">https://orcid.org/0000-0002-4787-1749</a>		<b>8. Performing Organization Report No.</b>	
<b>9. Performing Organization Name and Address</b> University of Wisconsin-Madison Department of Civil & Environmental Engineering 1415 Engineering Drive Madison, WI 53706		<b>10. Work Unit No.</b>	
		<b>11. Contract or Grant No.</b> Safety Research Using Simulation (SAFER-SIM) University Transportation Center (Federal Grant #: 69A3551747131)	
<b>12. Sponsoring Agency Name and Address</b> Safety Research Using Simulation University Transportation Center Office of the Secretary of Transportation (OST) U.S. Department of Transportation (US DOT)		<b>13. Type of Report and Period Covered</b> Final Research Report (June 2020 – May 2021)	
		<b>14. Sponsoring Agency Code</b>	
<b>15. Supplementary Notes</b> This project was funded by Safety Research Using Simulation (SAFER-SIM) University Transportation Center, a grant from the U.S. Department of Transportation – Office of the Assistant Secretary for Research and Technology, University Transportation Centers Program. <i>The contents of this report reflect the views of the authors, who are responsible for the facts and the accuracy of the information presented herein. This document is disseminated in the interest of information exchange. The report is funded, partially or entirely, by a grant from the U.S. Department of Transportation's University Transportation Centers Program. However, the U.S. government assumes no liability for the contents or use thereof.</i>			
<b>16. Abstract</b> Technology advancements in the past two decades have made the human-vehicle connection stronger than ever. Since 2009 there has been a boom in the development of autonomous vehicles (AVs) as an increasing number of manufacturers have begun to see immense potential in this area of artificial intelligence (AI). While the private sector is racing forward with the development of autonomous features, there is a need to understand how the human driver will interface with these features before Level 5 automation is finally achieved. This study sought to explore how distractions during automated driving impacted hazard anticipation upon re-taking control.			
<b>17. Key Words</b> Highways; Operations and Traffic Management; Safety and Human Factors		<b>18. Distribution Statement</b> No restrictions. This document is available through the <a href="#">SAFER-SIM website</a> , as well as the <a href="#">National Transportation Library</a>	
<b>19. Security Classif. (of this report)</b> Unclassified	<b>20. Security Classif. (of this page)</b> Unclassified	<b>21. No. of Pages</b> 41	<b>22. Price</b>

## Table of Contents

Table of Contents.....	vii
List of Figures .....	viii
List of Tables .....	ix
Abstract.....	x
1 Introduction and Background .....	1
2 Literature Review.....	3
2.1 Background of HCM Critical and Follow-Up Headways.....	3
2.2 Methods for Estimating Critical Headway.....	6
2.3 Factors Influencing Gap Acceptance Parameters .....	7
3 Data Collection .....	10
4 Methodology .....	12
4.1 Video Data Reduction .....	12
4.2 Mean Critical Headway Estimation.....	14
4.3 Mean Follow-Up Headway .....	15
4.4 Meta-Regression Analysis .....	16
4.5 Left Turn Saturation Flow.....	17
5 Results.....	18
5.1 Mean Critical and Follow-Up Headway .....	18
5.2 Meta-Regression Analysis Results.....	20
5.3 Saturation Flow Evaluation Results.....	23
6 Conclusions .....	27
References .....	29

## List of Figures

Figure 2.1 – HCM (a) Critical Headway by Intersection, (b) Aggregated Estimate .....	5
Figure 4.1 – Screenshot of Video Processing.....	12
Figure 4.2 – Illustration of Timestamps Obtained from Video Processing .....	13
Figure 5.1 – Critical and Follow-up Headways.....	20
Figure 5.2 – (a) Critical Headway and (b) Follow-up Headway Meta-Regression .....	23
Figure 5.3 – Saturation Flow for Every approach, HCM and Observed.....	24
Figure 5.4 – Difference of Saturation Flow from HCM Estimates .....	25
Figure 5.5– Saturation Flow Rate as a Function of Opposing Traffic and $S \times W / 1,000$ .....	26

## List of Tables

Table 4.1 – Descriptive Statistics .....	<b>Error! Bookmark not defined.</b>
Table 4.1 – Descriptive Statistics.....	11
Table 5.1 – Summary of Results .....	19



## **Abstract**

Critical and follow-up headways are the foundation for estimating the saturation flow of permissive left turns at signalized intersections. Current critical and follow-up headways recommended in the 2016 Highway Capacity Manual (HCM) are based on limited data collected from five intersections in Texas in the 1970s. This study analyzed over 2,500 left-turning vehicles at 45 intersection approaches, provides insights into gap acceptance parameters, and evaluates the effect of different site-specific factors. Video data were collected and processed from different geographical regions in the United States—Arizona, Florida, North Carolina, Virginia, and Wisconsin. Using the Maximum Likelihood method to estimate gap acceptance parameters, the mean critical headway was 4.87 seconds and the mean follow-up headway was 2.73 seconds. The mean critical headway for large vehicles was 6.03 seconds. To account for site-specific characteristics, the effect of several geometric and operational variables on critical and follow-up headway were explored. Through a meta-regression analysis, the posted speed limit and width of opposing travel lanes were found to have a significant effect on gap acceptance parameters. Results showed that with decreasing posted speed limit and width of opposing lanes, critical and follow-up headways also decrease resulting in greater saturation flows. When site-specific saturation flow estimates are compared with HCM saturation flow estimates, the differences ranged from -30% to +23%. This research quantifies and illustrates the impact of site-specific characteristics on gap acceptance parameters and saturation flow.

## 1 Introduction and Background

Drivers making permissive left-turning movements decide when it is safe to make the maneuver based on gaps available in opposing through traffic, right-turning traffic, presence of pedestrians or cyclists, and line of sight obstructions. Thus, driver behavior looking for acceptable and safe headways is commonly known as “gap acceptance.” Analytical procedures for estimation of permissive left-turn capacity and signal optimization rely on gap acceptance theory.

Two gap acceptance parameters are the foundation for estimating saturation flow: critical and follow-up headways. The 2016 Highway Capacity Manual (HCM) uses fixed values of 4.50 and 2.50 seconds for critical and follow-up headways respectively (NAS 2016). These HCM values are based on field data, collected in Texas in the 1970s, from three intersections for the critical headway and five intersections for the follow-up headway (Messer et al. 1975). The HCM critical and follow-up headway estimates do not account for geometric and operational measures; consequently, the saturation flow estimates do not reflect intersection site-specific characteristics. Current capacity estimation in the HCM includes several factors to adjust the “base” saturation flow that are intended to account for some operational factors such as heavy vehicles, parking, bus blockage, area type, lane utilization, presence of bicyclist and pedestrians, spillback, and work zones. However, intersection geometry, traveling speed, pedestrians crossing before (leading pedestrian interval) and during permissive movements are not considered. Past research has shown evidence of the impact of geometric and operational features on gap acceptance parameters (Devarasetty et al. 2012, Joshua and Saka 1992, Saka 1998, Yan and Radwan 2008, Ogallo and Jha 2014, Tian et al. 2000, Brilon 1988, Zohdy et al. 2010, Hutton et al. 2015, Hurwitz et al. 2013, Alhajyaseen et al. 2013). Thus, in this research, we focused on the impact of intersection geometry and posted speed limit on gap acceptance parameters and saturation flow.

Operational effects of permissive left-turns have been studied extensively over the last two decades (Knodler et al. 2007, Knodler et al. 2006, Knodler and Noyce 2005, Noyce et

al. 2007, Daily et al. 2019, Zheng et al. 2012). As a continuation of this research, field data was collected for over 2,500 left-turning vehicles from 45 intersection approaches with diverse configurations and from different geographical regions in the United States. Several potential predictor variables were explored to quantify the impact of site-specific characteristics on gap acceptance parameters and saturation flow compared to HCM recommended values.

## 2 Literature Review

The literature review includes a historical account of the development of the HCM critical and follow-up headways, methods for critical headway estimation, and effect of geometric and operational characteristics on gap acceptance parameters.

### 2.1 Background of HCM Critical and Follow-Up Headways

For signalized intersections with permissive left turns, the focus is on quantifying the maximum number of left turn vehicles that can be accommodated during the permissive phase, which is defined as the saturation flow rate (NAS 2016, Drew 1968):

$$S_p = \frac{V_o \times e^{\frac{-V_o \times T_{cg}}{3,600}}}{1 - e^{\frac{-V_o \times T_{fh}}{3,600}}} \quad (1)$$

Where,

$S_p$  = saturation flow rate of left turns with permissive indication (veh/h/ln);

$V_o$  = opposing flow rate (veh/h);

$T_{cg}$  = critical headway of 4.50 seconds;

$T_{fh}$  = follow-up headway of 2.50 seconds.

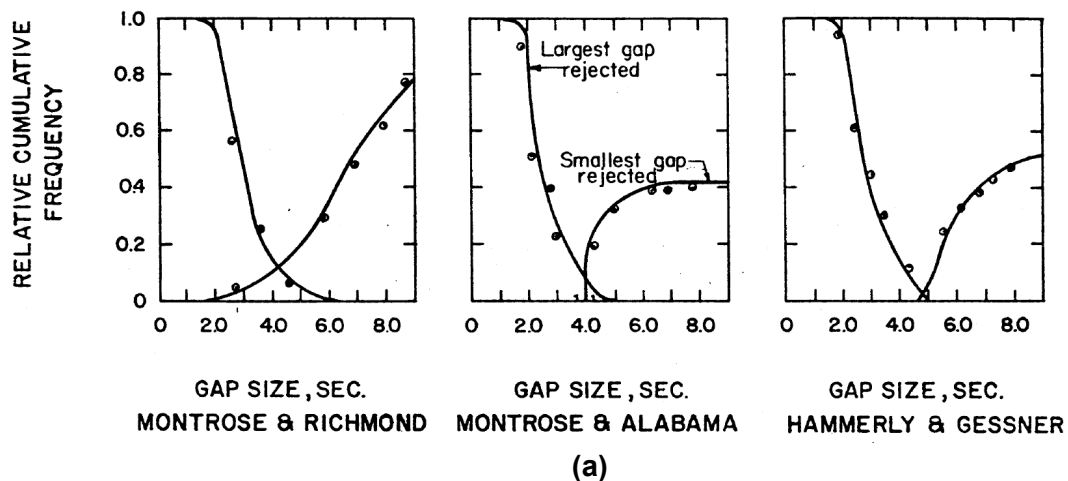
There are three major assumptions that go along with Equation 1 (Troutbeck and Brilon 2005):

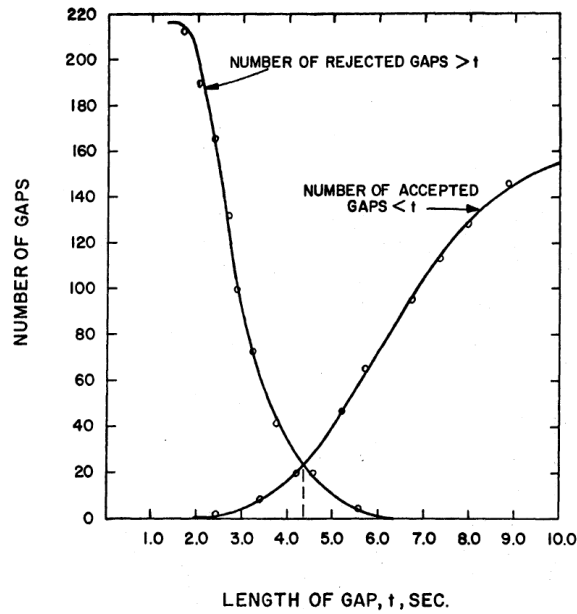
- a) Critical and follow-up headways are assumed to be constant for all drivers and are not represented by the mean of an observed distribution of drivers.
- b) Opposing traffic headways follow an exponential distribution.
- c) Each traffic stream flow rate is assumed to be constant and uniform.

The critical headway is the minimum time interval between two successive vehicles of opposing traffic that the left turn vehicle considers to cross opposing traffic and complete the maneuver. A headway shorter than the critical headway will be rejected and any headway greater in time duration accepted.

The follow-up headway is the time headway between vehicles in a queue accepting the same gap in opposing traffic. The follow-up headway is similar to the saturation headway at signalized intersections.

In 1975, Messer et al. (1975) led the research study titled “Effects of Design on Operational Performance of Signal Systems.” Using the methodological approach presented by Drew (1968), left-turn capacity of an intersection during free-flow conditions was evaluated. Messer et al. (1975) estimated the critical and follow-up headways using video tapes recorded at three and five intersections in Houston, Texas in 1974 and 1975, respectively. For the critical headway, all three intersections had one left turn approach with two opposing through lanes and used two-phase signals with permissive left turns. The specific number of observations is unknown, but data was collected for a total of 87 signal cycles. Through video processing, the largest headway rejected and the accepted for each left turning vehicle were collected. Based on Raff’s method (1950), graphs of relative cumulative frequency of largest rejected and accepted headways were evaluated to determine the intersection of curves and determine the approximate critical headway. Results of the critical headway estimates range between four to five seconds and are provided in Figure 2.1(a) (Messer et al. 1975). Observations from the three intersections were aggregated to estimate the overall critical headway as provided in Figure 2.1(b) (Messer et al. 1975).





(b)

**Figure 2.1 – HCM (a) Critical Headway by Intersection, (b) Aggregated Estimate  
(Messer et al. 1975)**

Based on the results obtained from data aggregation of three intersections, the observed critical headway was approximately 4.36 seconds. The value of 4.50 seconds for the critical headway was selected as a reasonable estimate for use in the left turn saturation flow rate (Messer et al. 1975). Similarly, the follow-up headway was estimated using data from five intersections. Two more intersections were included to the sites already used in the critical headway estimation. The overall number of follow-up observations was 311. Some issues with sample bias were identified since at two of the intersections, over one hundred observations (111 and 146) were recorded and the rest of intersections had 10, 15, and 29 observations. Individual follow-up headways ranged between 2.31 and 2.79 seconds. The aggregated mean follow-up headway was 2.48 seconds, which was rounded up to 2.50 seconds (Messer et al. 1975).

The critical headway of 4.50 seconds and follow-up headway of 2.50 seconds have been used and adopted in the HCM for many decades.

## 2.2 Methods for Estimating Critical Headway

Estimating critical headway is not a trivial task. There are numerous methods with different assumptions for estimating critical headway. Raff's method seems to be one of the earliest methods proposed for estimating critical headways (Raff 1950). However, estimation of critical headway with Raff's method and cumulative probability distributions is sensitive to traffic volumes. Raff's method should no longer be used in the estimation of reliable critical headways since more rigorous methods have been proposed ever since (Brilon et al. 1999).

Siegloch's method (Siegloch 1973) uses linear regression to represent the average headway size values using the number of vehicles that enter during this average headway size as the predictor variable. Siegloch's method is usually used for saturated conditions (Siegloch 1973). For undersaturated conditions, the lag method considers consistent drivers, independence of vehicle arrival times, and estimates the critical headway based on observed lags (Brilon et al. 1999). Ashworth's method (Ashworth 1968) assumes main stream headways are exponentially distributed, independence between consecutive headways, and normal distributions for accepted headways and critical headway. The average critical headway can be estimated from the mean and standard deviation of accepted headways (Ashworth 1968).

Harders' method (Harders 1968) is similar to the lag method, but only headways are included. However, there is no evidence of a mathematical procedure used to support the methodological approach (Brilon et al. 1999). There are also methods based on logit and probit procedures which allow the evaluation of other external effects on critical headway (Brilon et al. 1999, Cassidy et al. 1995, Miller 1971). However, logit and probit procedures provide very different results when only lags, only headways, or both are used, failing to provide consistent results (Brilon et al. 1999). Hewitt has also provided a series of procedures for estimating critical headways (Brilon et al. 1999, Hewitt 1971). In general terms, information required for each time interval are the total number of headways,

number of rejected headways, total number of lags, and number of rejected lags. A probit estimating procedure is used to obtain critical headway (Brilon et al. 1999, Hewitt 1971).

Selecting a reliable methodological approach for estimation of the critical headway is difficult since there are varied assumptions and processes. Brilon et al. (1999) compared the performance of several methods to estimate critical headway. One major consideration was that the process should not depend on traffic volume during the time of observation. A criterion for evaluation was developed based on gap/lag distribution, consistency, robustness, and capacity model compatibility. From the methods evaluated, the methods proposed by Troutbeck (2014) and Hewitt (1983) provided the best results based on the evaluation criteria. Both methods were valid for the scenarios studied and were recommended for application. Troutbeck's method of maximum likelihood (ML) optimization uses accepted and maximum rejected headways and assumes observations follow a log-normal distribution, to estimate critical headway (Troutbeck 2014).

Estimation of follow-up headway is not as complicated as critical headway and conventional arithmetic mean, variance, and normal distribution are accepted.

### 2.3 Factors Influencing Gap Acceptance Parameters

Several studies have evaluated geometric and operational factors that influence critical and follow-up headways. Devarasetty et al. (2012), through binary logit models, found that headway duration, total wait time, time to turn, distance to next signal downstream, and median type were significant factors in predicting the probability of accepting or rejecting headways. Lag duration, time to turn, crossing width, speed limit, and distance to next signal downstream were also found to be significant predictors of the probability of accepting or rejecting lags.

Issues have been long identified with vehicles in the opposing left-turn lane blocking the line of sight. From theoretical models, Joshua and Saka (1992) and Saka (1998) concluded that nonstationary objects at intersections increase left turn critical and follow-up headways. Using field data from one intersection in Orlando, Florida, Yan and Radwan



(2008) showed that sight-distance issues significantly increase critical and follow-up headways (Yan and Radwan 2008). Similarly, using field data from ten intersection in Baltimore and Annapolis, Maryland, Ogallo and Jha (2014) found that left turn obstruction increases critical and follow-up headways.

Tian et al. (2000) conducted a step-wise regression and found that major factors affecting critical and follow-up headways at unsignalized intersections include intersection geometry, vehicle type, approach grade, and traffic movements. Using the ML method and aggregated data from several intersections, critical headway of trucks (5.50 sec) was significantly larger and more variable than passenger vehicles (4.10 sec). Similarly, follow-up headway for trucks (3.10 sec) was larger than passenger vehicles (2.20 sec). It was also observed that the ratios of follow-up time and critical headway ranged between 0.40 and 0.90, with the majority around 0.60. Similar to previous results provided by Brilon (1988).

Zohdy et al. (2010) used logistic regression with predictor variables of gap duration, wait time for acceptable headways, time traveled to clear a conflict point, and rain intensity. Data were obtained during two months at an intersection in Christiansburg, Virginia. Results showed that acceptable headways decrease as a function of waiting time and increase as rain intensity increases.

Using naturalistic data, Hutton et al. (2015) evaluated gap acceptance behavior of drivers at left-turn lanes with negative, zero, or positive offsets. The study evaluated 269 left-turn maneuvers at signalized intersections with permissive phase. Logistic regression was used to estimate the critical headway for drivers as a function of offset and presence of vehicles in the opposing left turn. Critical headways were longer at intersections with negative offsets than at those with zero or positive offsets. The critical headway was longer when vehicles were present in the opposing left turn lane (Hutton et al. 2015). In a driver simulation study using eye tracking technology, Hurwitz and Monsere (2013) evaluated the effects of opposing traffic, the presence and walking direction of pedestrians, and flashing yellow arrow indication on left turn driver performance. The results of the study

showed that drivers paid more attention with increasing presence of pedestrians. Alhajyaseen et al. (2013) also analyzed gap acceptance behavior of left turning vehicles and the presence of pedestrians at signalized intersections. The results of the study indicate that drivers tend to accept shorter headways between near-side pedestrians compared to far-side pedestrians.

In summary, the methodological approach and assumptions significantly influence the magnitude of critical and follow-up headways. There is evidence of the effect of geometric and operational factors on gap acceptance parameters. Limited field data has been used to study gap acceptance parameters at signalized intersections.

### 3 Data Collection

Video recordings of left turn maneuvers, opposing traffic, and traffic signal indication at urban signalized intersections with permissive or protected/permissive left turns were used in this study. Through outreach to several public and private agencies across the United States, the research team obtained and collected about 500 hours of video data at 27 intersections between 2016 and 2019, from three different geographical regions in the United States— East (Florida, North Carolina, Virginia), Midwest (Wisconsin), and West/Southwest (Arizona). Based on the geometric characteristics, video field of view, one or multiple left turn approaches at each intersection were used, resulting in 45 approaches for analysis. Using aerial and street view images, geometric and operational configuration such as number of lanes, offset, median widths, lane widths, and posted speed limit were collected. Table 4.1 provides additional details for study locations including the total width in feet of opposing traffic lanes (through and right turn lanes) and posted speed limits.

A minimum of three intersections were selected from each geographic region. Intersections had diverse geometric and operational conditions. One approach had dual left turn lanes and the rest had one left turn lane. Opposing through traffic lanes ranged between one and three. Approaches had none or one exclusive right turn lane. Width of opposing traffic lanes ranged between 13 to 45 ft. Posted speed limit ranged between 25 and 55 mph.

**Table 4.1 – Descriptive Statistics**

No.	Intersection	App.	City	State	Left Turn Lanes	Opposing Lanes			Speed Limit (mph)
						Through	Right	Width (ft)	
1	24th St and Thomas Rd	EB	Phoenix	AZ	1	2	0	20	35
2	24th St and Thomas Rd	NB	Phoenix	AZ	1	2	0	20	35
3	24th St and Thomas Rd	SB	Phoenix	AZ	1	2	0	30	35
4	44th St and Camelback Rd	EB	Phoenix	AZ	1	3	0	32	40
5	44th St and Camelback Rd	WB	Phoenix	AZ	1	3	0	32	40
6	44th St and Camelback Rd	SB	Phoenix	AZ	1	3	0	30	40
7	Chandler Blvd and Rural Rd	WB	Chandler	AZ	1	3	0	38	45
8	Hartwood M. Rd and Hancock Rd	EB	Clermont	FL	1	1	1	23	40
9	Hooks St and Hancock Road	NB	Clermont	FL	1	1	1	27	25
10	Johns Lake Rd and Hancock Rd	NB	Clermont	FL	1	1	0	14	45
11	US-27 and Hook St	EB	Clermont	FL	1	1	1	28	40
12	US-27 and Hook St	WB	Clermont	FL	1	1	0	23	30
13	Eastchester Dr and Penny Rd	NB	High Point	NC	1	2	1	33	45
14	NC-68 and Willard Dairy Rd	SB	High Point	NC	1	2	1	36	40
15	NC-54 and Highgate Dr	WB	Durham	NC	1	1	0	14	45
16	NC-42 and Cleveland Rd	EB	Garner	NC	1	1	1	28	45
17	NC-42 and Cleveland Rd	WB	Garner	NC	2	2	0	35	45
18	Broad Ave and Long Dr	EB	Rockingham	NC	1	2	1	36	45
19	Washington St and Long Dr	NB	Rockingham	NC	1	1	0	16	35
20	Washington St and Long Dr	SB	Rockingham	NC	1	1	0	15	35
21	New Hope Rd and Redbud Dr	EB	Gastonia	NC	1	2	0	23	35
22	New Hope Rd and Redbud Dr	NB	Gastonia	NC	1	2	0	24	35
23	Ebert Rd and Clemmonsville Rd	EB	Winston-Salem	NC	1	1	0	13	45
24	Ebert Rd and Clemmonsville Rd	WB	Winston-Salem	NC	1	1	0	13	45
25	Forestville Rd and Rogers Rd	WB	Wake Forest	NC	1	1	1	27	35
26	Forestville Rd and Rogers Rd	SB	Wake Forest	NC	1	2	0	28	45
27	Lebanon Rd and Lawyers Rd	EB	Mint Mill	NC	1	1	1	23	45
28	Lebanon Rd and Lawyers Rd	WB	Mint Mill	NC	1	1	1	20	45
29	Lebanon Rd and Lawyers Rd	NB	Mint Mill	NC	1	1	0	25	35
30	Lebanon Rd and Lawyers Rd	SB	Mint Mill	NC	1	1	0	17	35
31	Gum Branch Rd and Indian Dr	EB	Jacksonville	NC	1	2	0	24	45
32	NC-49 and Zion Church Rd	EB	Concord	NC	1	2	1	36	55
33	NC-49 and Zion Church Rd	WB	Concord	NC	1	2	1	40	55
34	NC-49 and Queens Dr	EB	Concord	NC	1	2	1	44	55
35	NC-49 and Queens Dr	WB	Concord	NC	1	2	1	44	55
36	NC-49 and Central Heights Dr	EB	Concord	NC	1	2	1	44	55
37	NC-49 and Central Heights Dr	WB	Concord	NC	1	2	1	43	55
38	Gordon Rd and White Rd	EB	Wilmington	NC	1	1	1	24	45
39	Waxpool Rd and Farmwell Rd	EB	Ashburn	VA	1	2	1	45	45
40	Waxpool Rd and Farmwell Rd	WB	Ashburn	VA	1	2	1	34	45
41	Wisconsin Ave and Meade St	EB	Appleton	WI	1	2	0	23	25
42	Northland Ave and Bennett St	EB	Appleton	WI	1	2	1	34	40
43	Northland Ave and Mason St	WB	Appleton	WI	1	2	1	34	40
44	Northland Ave and Meade St	NB	Appleton	WI	1	2	0	22	30
45	Northland Ave and Meade St	WB	Appleton	WI	1	2	1	36	40

Notes: App. = approach; Width (ft) = width of opposing through and right turn lanes; Speed Limit (mph) = posted speed limit.

## 4 Methodology

This section describes video data processing approach, statistical modeling, and analytical evaluation. The focus of this study is to evaluate the variability of left turn critical and follow-up headways and their effect on left turn saturation flow at signalized intersections with permissive or protected/permissive indication.

### 4.1 Video Data Reduction

Video processing consisted of collecting timestamps for left turning, opposing through, and right turning vehicles during the permissive phase. Left turn maneuvers that occurred during the protected or end of green phase were not considered. Figure 4.1 provides an example of the video processing set up. Approaches, stop bars, and traffic signal indication had to be clearly identified and visible in the field of view of the camera.

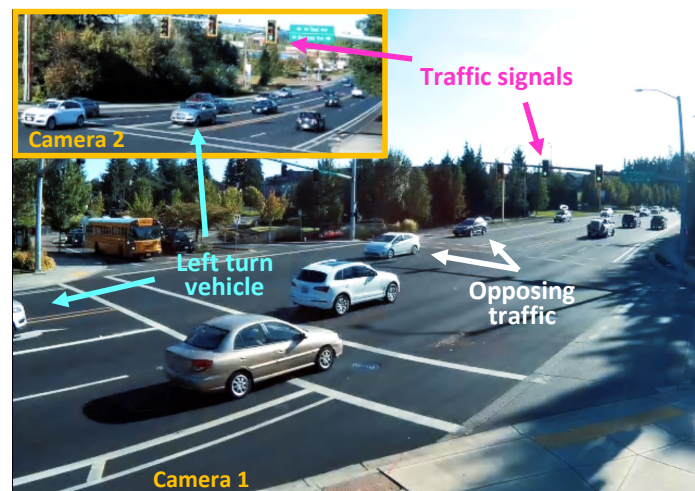


**Figure 4.1 – Screenshot of Video Processing**

Timestamps were collected at different locations for left turn and opposing vehicles. Figure 4.2 illustrates the sequence of a left turn maneuver with opposing traffic and different timestamps collected. Two timestamps were recorded for each left turn maneuver— $l_0$  and  $l_1$ . The first timestamp  $l_0$  was recorded when left turn vehicles arrived or crossed the left turn lane stop bar, time in which left turning vehicles were actively seeking and waiting for an acceptable headway. The second timestamp  $l_1$  was recorded when left turn vehicles proceeded to cross over opposing traffic lanes. The location of  $l_1$

had some variability since locations at which vehicle accepted headways depended on waiting time, approaching speed, and driving behavior. Thus,  $l_1$  was considered the time and location where left turn vehicles crossed the opposing through traffic. Timestamp  $t_i$  ( $i=0, 1, \dots, n$ ) were recorded for opposing traffic when vehicles crossed the stop bar which served to calculate headways. Video player software with decimal second time precision was used to accurately record timestamps and rewind/skip video frames. Timestamps were recorded in a spreadsheet developed to flag any potential errors, process headway information, index, and validate the data. The spreadsheet provided a detailed distribution of headways associated with each left turn vehicle, type of headway (lag or gap), calculated follow-up headways, and identified the largest rejected and accepted headway.

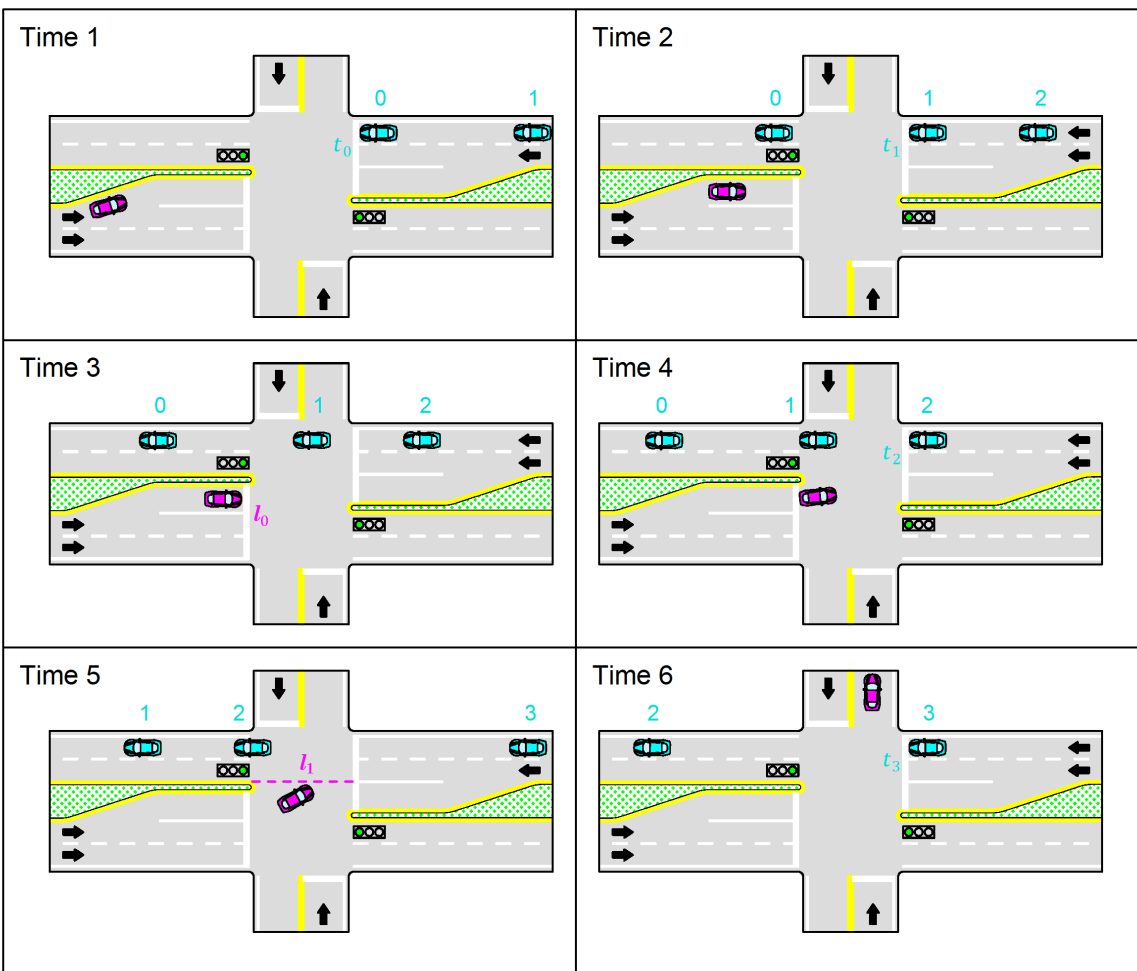


**Figure 4.2 – Illustration of Timestamps Obtained from Video Processing**

Accepted and largest rejected headways were used to estimate critical headway using Troutbeck's method (Troutbeck 2014) which provides reasonable estimates with 25 to 30 observations compared to other methods. Since every timestamp was recorded manually, a significant effort was required for video processing and validation. Data was collected for left turning passenger vehicles and large vehicles—single unit trucks, buses, and semi-trucks. Also, there was a significant amount of video available, so it was not feasible to process all video. Videos were processed for 7-10 AM and 3-6 PM hours during weekdays. These periods of analysis were selected to optimize video processing and maximize the number of observations collected. On average, it took approximately three hours to process and validate one hour of video. Therefore, at least 25 left turn observations by approach were collected. Overall, timestamps for over 2,500 left turn observations and close to 15,000 opposing through vehicles were collected, which resulted from processing over 145 hours of video.

There were some special cases with pedestrians and possibly distracted drivers that influenced gap acceptance behavior. In the few observed cases with pedestrians, drivers were more conservative accepting gaps or in some cases made slow maneuvers when pedestrians were on the sidewalk or crosswalk intersecting the left turn trajectory. Similarly, some erratic drivers that rejected large gaps and waited for prolonged periods were observed which in part may be attributed to driver distraction. Data from special cases were not considered in the analysis of this report due to the limited number of observations, but should be a topic of interest for future research efforts as more data becomes available.

#### 4.2 Mean Critical Headway Estimation

Methods recommended for practical application are the ML method from Troutbeck (2014) and the method developed by Hewitt (1983). For this study, mean critical headway was estimated using gaps, lags, and the ML method. The ML method considers that a driver's ( $i$ ) critical headway is greater than the largest rejected headway ( $r_i$ ) and smaller than the

accepted headway ( $a_i$ ). The assumption made is that critical headways follow a lognormal probability distribution, which is skewed and has non-negative values. Therefore, the probability of a driver's critical headway between  $r_i$  and  $a_i$  is the difference between the corresponding headways' cumulative distribution functions  $F(r_i) - F(a_i)$ . By adding all observed drivers' probability headway estimates, the logarithm likelihood of a sample of  $n$  drivers, presented in Equation 2, was used to estimate the mean and variance of the critical headway through ML optimization (Troutbeck 2014). A spreadsheet was developed to estimate mean critical gap and variance through Excel solver optimization. The critical headway was computed for individual approaches as well as an aggregated estimate for all approaches.

$$L = \sum_{i=1}^n \ln[F(a_i) - F(r_i)] \quad (2)$$

#### 4.3 Mean Follow-Up Headway

The follow-up headway is the time headway between vehicles in a queue taking the same gap in opposing traffic. Usually queued vehicles follow a lead vehicle and the following vehicles maintain a distance to determine if the headway accepted by the vehicle in front is still acceptable. The follow-up headway is similar to the saturation headway at signalized intersections. Some considerations were taken to determine a follow-up headway in this study:

- Following-up vehicles should be in the queue when the lead or vehicle in front accepts a headway.
- Following-up vehicles with a lead vehicle that accepted a lag were not considered. Usually, these follow-up vehicles approached the intersection without stopping and maintaining a distance with the lead vehicle and accepting the same lag.
- Following-up vehicles that did not short cut the trajectory of the lead or vehicle in front. Following-up vehicles may significantly shorten the left turn trajectory, cross



over opposing lanes earlier than the lead vehicle, and in some cases take a position in parallel with the lead vehicle or even take over.

- Following-up vehicles during the protected indication or end of green phase were not considered.

In general terms, obtaining accurate and well-defined follow-up headways is difficult. Thus, video processing, selection, and validation required an additional effort to guarantee its accuracy. The mean follow-up headway was obtained with the standard arithmetic mean with corresponding variance for all approaches. An aggregated follow-up headway estimate was also obtained.

#### 4.4 Meta-Regression Analysis

Conventional regression modeling assesses the relationship between one or more covariates and a dependent variable. Similarly, the same approach can be used with meta-analysis, but the difference is that covariates are at the level of the study rather than the level of the subject. The dependent variable is the effect size in the studies rather than subject scores. Meta-regression analysis includes the same principles of effect size, precision, study weights, and statistical significance as conventional meta-analysis (Borenstein 2021). Thus, in this study, the mean, variance, and number of observations of critical and follow-up headways of every approach were used to conduct a meta-regression analysis using geometric and operational features as predictor variables. The methodological approach and goodness of fit addressed heteroscedasticity, heterogeneity, residual heterogeneity, and moderators. Meta-regression was conducted using mixed effects with the Metafor package in R (Viechtbauer 2010). The following predictor variables were explored:

- Distance between left turn stop bar and opposing through stop bar (ft).
- Left turn offset.
- Left turn trajectory length (distance from stop bar to clear all opposing lanes) (ft).
- Median width (ft).

- Number of opposing right turn lanes.
- Number of opposing through lanes.
- Total number of opposing lanes.
- Posted speed limit (mph).
- Wait time (sec).
- Width of opposing lanes (ft).
- Left turn vehicle type.

The objective of using meta-regression analysis was to estimate critical and follow-up headways as a function of site-specific geometric and operational characteristics for estimation of saturation flow and capacity. Presence of pedestrians and obstruction of line of sight were not considered in the analysis due to limited observations of these special cases.

#### 4.5 Left Turn Saturation Flow

For left turns at intersections with permissive indication, the saturation flow rate is the maximum number of vehicles traversing opposing traffic and completing left turn movements during the permissive interval for every signal cycle during an hour and under prevailing traffic conditions. The HCM defines the saturation flow for left turns with permissive indication with Equation 1 covered extensively in the literature review section (NAS 2016, Drew 1968).

## 5 Results

Critical headway estimates, using the ML proposed by Troutbeck, and follow-up headway estimates are provided. Meta-regression models are provided separately for critical and follow-up headways. Based on the results, the effect of site-specific characteristics on gap acceptance parameters and the impact on the saturation flow are illustrated.

### 5.1 Mean Critical and Follow-Up Headway

Results of critical and follow-up headways are provided in Table 5.1. The results include the number of observations, mean critical headway, mean follow-up headway, and standard deviation in parentheses.

Observations of the critical headway ranged between 25 and 83 left turns with a total of 2,108 observations. Mean critical headway estimates ranged between 3.68 and 6.41 seconds. The aggregated mean critical headway was 4.87 seconds with a standard deviation of 1.54 seconds. Limited number of left turn observations were available for large vehicles. There were only 18 left turn observations involving large vehicles (2 school buses, 12 single unit trucks, and 4 semi-trucks). The mean critical headway for large vehicles was 6.03 seconds with a standard deviation of 1.37 seconds. Despite the limited number of observations, the mean critical headway for large vehicles is different than the aggregated estimate of 4.87 seconds which only included passenger vehicles. Thus, in line with previous research, large vehicles require longer gaps to complete left turn maneuvers with permissive indication.

At some intersection approaches, follow-up headway observations were scarce, so limited or no observations were recorded at those locations. For approaches with observations, there were between 3 to 40 follow-up vehicles with a total of 472 observations which were sufficient for analysis. Mean follow-up headway estimates ranged between 2.03 and 4.36 seconds. The aggregated mean follow-up headway was 2.73 seconds with corresponding standard deviation of 0.97 seconds.

**Table 5.1 – Summary of Results**

No.	Intersection	App.	City	State	CH <sub>obs</sub> <sup>1</sup>	CH (sec) <sup>1</sup>	FH <sub>obs</sub> <sup>2</sup>	FH (sec) <sup>2</sup>
1	24th St and Thomas Rd	EB	Phoenix	AZ	50	5.48(1.87)	14	2.82(0.62)
2	24th St and Thomas Rd	NB	Phoenix	AZ	50	5.27(1.68)	11	2.75(0.55)
3	24th St and Thomas Rd	SB	Phoenix	AZ	50	5.09(2.26)	13	3.21(1.06)
4	44th St and Camelback Rd	EB	Phoenix	AZ	42	5.84(2.85)	6	2.30(0.34)
5	44th St and Camelback Rd	WB	Phoenix	AZ	44	5.47(3.11)	5	3.11(1.24)
6	44th St and Camelback Rd	SB	Phoenix	AZ	44	5.31(1.08)	10	3.35(1.01)
7	Chandler Blvd and Rural Rd	WB	Chandler	AZ	46	5.90(1.21)	7	3.18(0.93)
8	Hartwood M. Rd and Hancock Rd	EB	Clermont	FL	50	4.36(1.61)	15	2.36(0.75)
9	Hooks St and Hancock Road	NB	Clermont	FL	51	4.01(1.05)	17	2.19(0.58)
10	Johns Lake Rd and Hancock Rd	NB	Clermont	FL	50	4.73(0.96)	9	2.54(0.59)
11	US-27 and Hook St	EB	Clermont	FL	26	4.26(1.21)	7	2.24(0.58)
12	US-27 and Hook St	WB	Clermont	FL	31	3.77(1.23)	8	2.03(0.86)
13	Eastchester Dr and Penny Rd	NB	High Point	NC	50	4.39(1.13)	22	2.89(1.21)
14	NC-68 and Willard Dairy Rd	SB	High Point	NC	38	3.85(0.73)		
15	NC-54 and Highgate Dr	WB	Durham	NC	59	5.14(0.53)	14	2.81(1.07)
16	NC-42 and Cleveland Rd	EB	Garner	NC	30	5.21(0.76)		
17	NC-42 and Cleveland Rd	WB	Garner	NC	50	4.68(0.95)	6	2.83(1.24)
18	Broad Ave and Long Dr	EB	Rockingham	NC	41	5.69(1.60)	5	3.24(1.69)
19	Washington St and Long Dr	NB	Rockingham	NC	45	3.77(0.99)		
20	Washington St and Long Dr	SB	Rockingham	NC	25	4.93(1.13)		
21	New Hope Rd and Redbud Dr	EB	Gastonia	NC	42	4.67(1.29)	15	2.73(0.84)
22	New Hope Rd and Redbud Dr	NB	Gastonia	NC	61	3.68(1.41)	22	2.39(0.78)
23	Ebert Rd and Clemmonsville Rd	EB	Winston-Salem	NC	43	4.87(2.04)	15	2.95(1.34)
24	Ebert Rd and Clemmonsville Rd	WB	Winston-Salem	NC	53	4.82(1.81)	19	2.44(1.23)
25	Forestville Rd and Rogers Rd	WB	Wake Forest	NC	50	5.09(1.63)	12	2.65(0.81)
26	Forestville Rd and Rogers Rd	SB	Wake Forest	NC	50	4.23(1.69)	16	2.77(0.47)
27	Lebanon Rd and Lawyers Rd	EB	Mint Mill	NC	51	3.95(1.17)	11	2.66(0.82)
28	Lebanon Rd and Lawyers Rd	WB	Mint Mill	NC	83	5.76(1.54)	26	2.46(0.95)
29	Lebanon Rd and Lawyers Rd	NB	Mint Mill	NC	40	4.34(1.61)	13	2.26(0.64)
30	Lebanon Rd and Lawyers Rd	SB	Mint Mill	NC	30	4.69(1.40)	4	2.44(0.22)
31	Gum Branch Rd and Indian Dr	EB	Jacksonville	NC	50	4.82(1.93)	8	2.60(0.56)
32	NC-49 and Zion Church Rd	EB	Concord	NC	39	5.32(1.49)		
33	NC-49 and Zion Church Rd	WB	Concord	NC	48	4.77(0.95)		
34	NC-49 and Queens Dr	EB	Concord	NC	50	4.46(0.92)	3	3.39(1.24)
35	NC-49 and Queens Dr	WB	Concord	NC	50	5.89(0.32)	4	4.36(0.92)
36	NC-49 and Central Heights Dr	EB	Concord	NC	50	5.15(1.27)	5	2.83(1.34)
37	NC-49 and Central Heights Dr	WB	Concord	NC	50	6.22(0.95)	7	2.98(0.74)
38	Gordon Rd and White Rd	EB	Wilmington	NC	51	4.98(1.20)	5	3.23(1.01)
39	Waxpool Rd and Farmwell Rd	EB	Ashburn	VA	50	4.98(0.89)	10	2.09(0.43)
40	Waxpool Rd and Farmwell Rd	WB	Ashburn	VA	50	5.65(1.71)	7	3.58(1.11)
41	Wisconsin Ave and Meade St	EB	Appleton	WI	46	6.41(0.62)	40	2.86(0.80)
42	Northland Ave and Bennett St	EB	Appleton	WI	49	5.18(0.84)	4	2.59(0.24)
43	Northland Ave and Mason St	WB	Appleton	WI	51	4.74(1.30)	15	3.33(1.19)
44	Northland Ave and Meade St	NB	Appleton	WI	52	4.53(0.96)	23	2.99(1.20)
45	Northland Ave and Meade St	WB	Appleton	WI	50	4.71(1.01)	19	2.63(0.97)
<b>All Approaches</b>					<b>2,108</b>	<b>4.87(1.54)</b>	<b>472</b>	<b>2.73(0.97)</b>

 Notes: <sup>1</sup> CH<sub>obs</sub>, CH=observations and critical headway; <sup>2</sup> FH<sub>obs</sub>, FH=observations and follow-up headway; St. deviation in parenthesis.

Figure 5.1 graphically illustrates individual estimates of critical and follow-up headways for all approaches and aggregated estimates compared to the HCM estimates. Aggregated estimates of this study were higher (statistically significant) than the HCM estimates—verified using generalized p-value test for critical headway and t-test for follow-up headway. As discussed previously, there is a wide range of values observed (in some cases due to limited observations) and aggregated estimates such as the HCM values do not reflect site-specific characteristics. The following section presents the results of the meta-regression analysis accounting for geometric and operational characteristics.

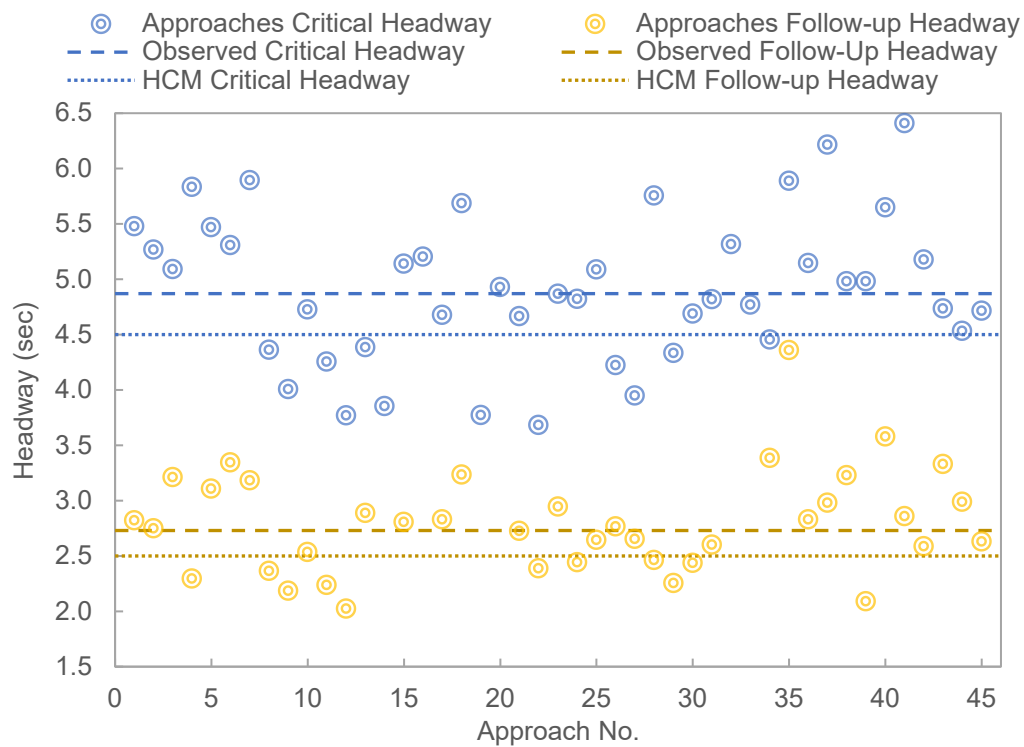


**Figure 5.1 – Critical and Follow-up Headways**

Notes: HCM=Highway Capacity Manual; Observed=aggregated study estimates.

## 5.2 Meta-Regression Analysis Results

Predictor variables considered for the analysis included several geometric and operational measures such as number of lanes, offset, median width, speed, and vehicle type. However, through a correlation analysis, opposing number of lanes, posted speed limit, and width of opposing lanes were found relevant to be included in the models. Correlation coefficients of selected variables are presented in Table 5.2. Correlation

coefficients between critical and follow-up headways were only provided for reference and were not considered as predictor variables for modeling. The opposing number of through lanes had a correlation factor of 0.45 with critical and follow-up headways. Similarly, posted speed limit had a correlation factor of 0.30 with the critical headway and 0.48 with the follow-up headway. The stop to stop distance refers to the distance from the left turn stop bar to the opposing through traffic stop bar. The stop to stop distance had a moderate association with critical and follow-up headways; however, it was also correlated to the posted speed limit.

**Table 5.2 – Correlation Analysis Results**

Description	CH	FH	Median Width	Offset	Stop to Stop Distance	Opposing Through Lanes	Opposing Right Turn Lanes	Width Opposing Lanes (W)	Posted Speed Limit (S)	S×W
CH <sup>1</sup>	1.00	0.43	0.09	0.23	-0.39	0.45	-0.02	0.22	0.26	0.30
FH <sup>2</sup>	0.43	1.00	0.07	0.16	-0.42	0.45	0.07	0.29	0.44	0.48
Median Width	0.09	0.07	1.00	0.57	-0.01	0.05	0.26	0.49	0.32	0.56
Offset	0.23	0.16	0.57	1.00	-0.09	0.49	0.29	0.62	0.30	0.60
Stop to Stop Distance	-0.39	-0.42	-0.01	-0.09	1.00	-0.10	0.00	0.02	-0.43	-0.16
Opposing Through Lanes	0.45	0.45	0.05	0.49	-0.10	1.00	-0.21	0.57	0.11	0.47
Opposing Right Turn Lanes	-0.02	0.07	0.26	0.29	0.00	-0.21	1.00	0.51	0.35	0.52
Width Opposing Lanes (W)	0.22	0.29	0.49	0.62	0.02	0.57	0.51	1.00	0.42	0.93
Posted Speed Limit (S)	0.26	0.44	0.32	0.30	-0.43	0.11	0.35	0.42	1.00	0.71
S×W	0.30	0.48	0.56	0.60	-0.16	0.47	0.52	0.93	0.71	1.00

Notes: <sup>1</sup> CH=critical headway; <sup>2</sup> FH=follow-up headway.

Although the correlation analysis showed evidence of association of the dependent variables with the number of opposing through lanes, it was not practical to include it as a predictor variable because of its limited ordinal integer nature and range (one to three). In addition, it does not effectively capture the presence of exclusive right turn lanes. Thus,

the predictor variable width of opposing lanes ( $W$ ), a continuous variable with a wider range of values, was selected for modeling as predictor variable along with the posted speed limit ( $S$ ). An interaction factor of the two selected variables ( $S \times W$ ) was also considered since it provided reasonable correlation coefficients for both critical and follow-up headways (0.30 and 0.48). Using the mean critical and follow-up headways, corresponding variance, and number of observations for each of the 45 approaches, a meta-regression was conducted using mixed effects with the Metafor package in R (Viechtbauer 2010). Table 5.3 provides the model coefficients, standard deviation, p-value, and confidence intervals. The model intercept and coefficients of the interaction term  $S \times W$  were found statistically significant at the 0.05 and 0.10 confidence level.

**Table 5.3 – Meta-Regression Model Coefficients**

Model	Variable	Estimate	St. Error	p-value	CI-lb <sup>4</sup>	CI-ub <sup>5</sup>
CH <sup>1</sup>	Intercept	4.16	0.36	<.001	3.46	4.86
	$S \times W^3$	0.66	0.22	0.003	0.23	1.08
FH <sup>2</sup>	Intercept	2.19	0.26	<.001	1.68	2.71
	$S \times W^3$	0.39	0.23	0.091	-0.06	0.84

Note: <sup>1</sup> CH=critical headway; <sup>2</sup> FH=follow-up headway; <sup>3</sup> S=posted speed limit, W=width of opposing lanes; <sup>4,5</sup> CI=confidence interval, lb=lower bound, ub=upper bound.

Figure 5.2 illustrates observed data and fitted model. Measures of goodness of fit were found satisfactory in terms of heterogeneity, residual heterogeneity, and moderators. The results of the meta-regression analysis provide intuitive estimates. For instance, with higher speeds and/or wider width of opposing lanes, the larger the critical and follow-up headways—with almost twice as much increase per unit of the interaction term  $S \times W/1,000$  for critical headway with an increase per unit of 0.66 second compared to 0.39 second for follow-up headway. The minimum and maximum observed values of  $S \times W/1,000$  were 0.53 and 2.42, which correspond to pairs of  $S=35$  mph,  $W=15$  ft and  $S=55$  mph,  $W=44$  ft, respectively.

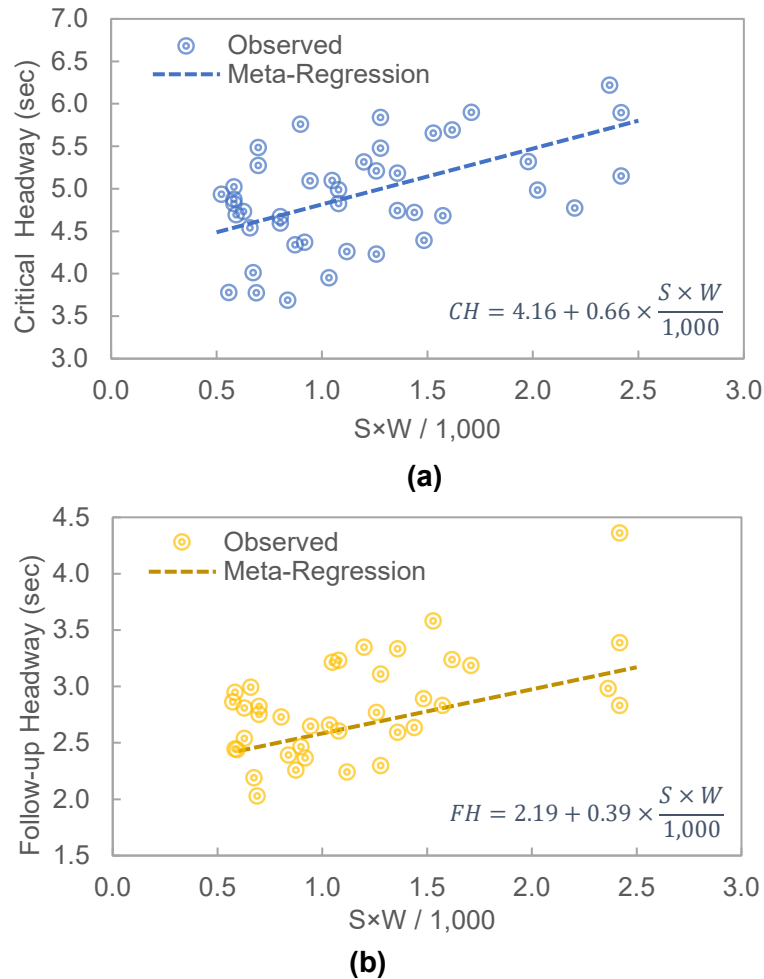


**Figure 5.2 – (a) Critical Headway and (b) Follow-up Headway Meta-Regression**

Notes: CH=critical headway; FH=follow-up headway; S=posted speed limit; W=width of opposing lanes.

### 5.3 Saturation Flow Evaluation Results

Saturation flow is an essential component in the process of estimating capacity at signalized intersections. Thus, the accuracy of HCM's saturation flow estimates is very important and highly dependent on critical and follow-up headways. Most micro- and macrosimulation software use these parameters for signal optimization and modeling. It is worth reminding that critical and follow-up headway estimates in the HCM were developed in 1975 with a methodological approach based on Raff's method and with three and five intersections in Houston, Texas, respectively (Messer et al. 1975).

Figure 5.3 provides saturation flow estimates, in gray, for all 45 approaches using their corresponding critical and follow-up headways. From all approaches, the maximum and minimum saturation flow curves were identified—these estimates are not confidence



intervals. The saturation flow with HCM recommended values and observed aggregated critical and follow-up headways are also provided.

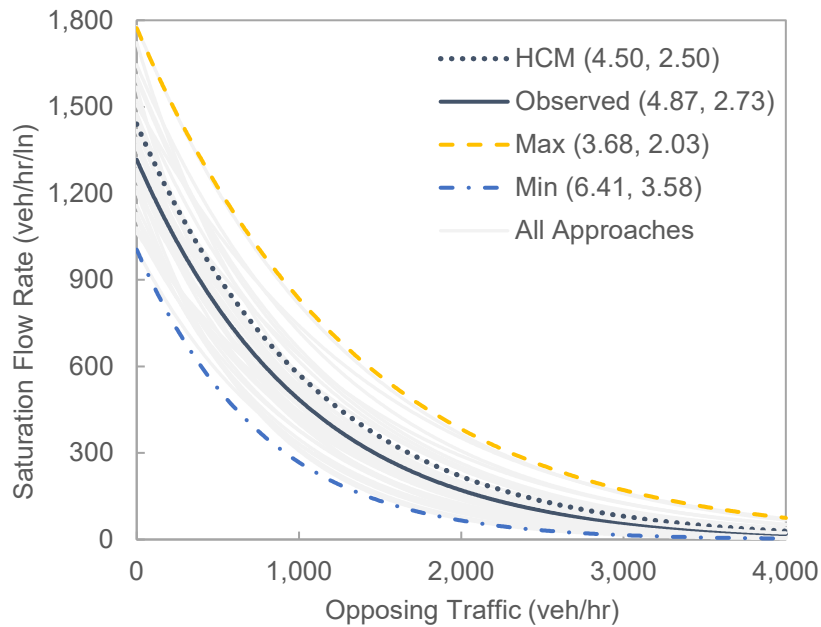


**Figure 5.3 – Saturation Flow for Every approach, HCM and Observed Estimates, and Min/Max Observed**

Notes: HCM=Highway Capacity Manual; Max=maximum observed, Min=minimum observed; Observed=aggregated study estimates; critical and follow-up headways in parenthesis.

The results show that there is a wide range in estimates of saturation flow that are quite different from the saturation flow estimates using HCM values. Figure 5.4 shows the magnitude of the difference in saturation flow. The results show that the maximum saturation flow had 333, 263, and 164 veh/hr/ln more than the HCM saturation flow at 0, 1,000, and 2,000 veh/hr of opposing traffic. The minimum saturation flow had 434, 305, and 153 veh/hr/ln less than the HCM saturation flow at 0, 1,000, and 2,000 veh/hr of opposing traffic. And, the saturation flow with observed aggregated headway estimates had 123, 87, and 48 veh/hr/ln less than the HCM saturation flow at 0, 1,000, and 2,000 veh/hr of opposing traffic.

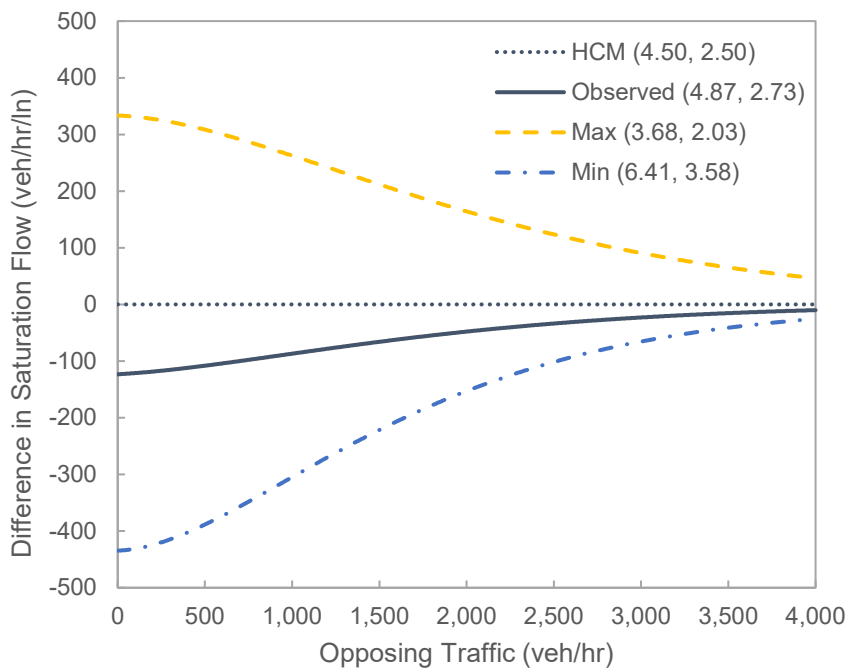


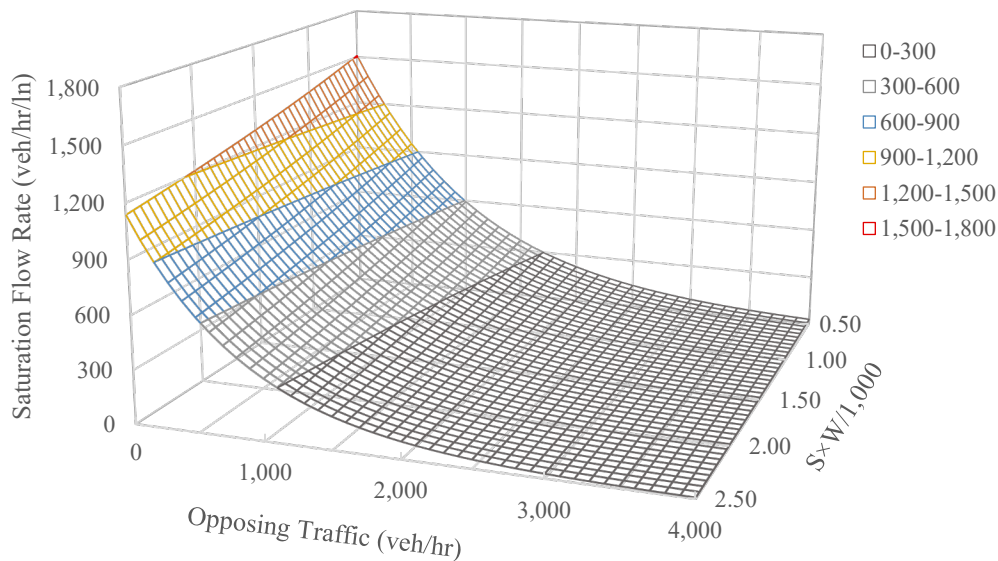
**Figure 5.4 – Difference of Saturation Flow from HCM Estimates**

Notes: HCM=Highway Capacity Manual; Max=maximum observed, Min=minimum observed; Observed=aggregated study estimates; critical and follow-up headways in parenthesis.

HCM and observed estimates of this study were both obtained from aggregated estimates that do not reflect site-specific characteristics. Assuming that one set of critical and follow-up headway aggregated estimates can be confidently applied to all scenarios is not accurate—even with data from multiple geographical regions in the United States and diverse geometric/operational conditions. Although the HCM introduces several factors to adjust the base saturation flow later in the capacity estimation process, the root of the estimate is in the critical headway, follow-up headway, and opposing traffic. The HCM applies multiple adjustment factors to the base saturation flow; however, intersection geometry or speed limits are not addressed. Also, implementing adjusting factors to the base saturation flow is not practical since the effect of interactions among factors is not properly understood nor addressed. Introducing site-specific characteristics to the computation of the saturation flow rate should be considered since the results of the meta-regression analysis in this study showed statistically significant predictor variables such as the posted speed limit and width of opposing traffic lanes. Many other studies have

also showed evidence of the effect of geometric and operational intersection features in headway estimates.

Meta-regression models presented in this research are a function of the posted speed limit and width of opposing traffic ( $S \times W/1,000$ ). Thus, the saturation flow can be directly evaluated as a function of these predictor variables and opposing traffic flow as illustrated in Figure 5.5. The results show that with a decreasing value of  $S \times W/1,000$ , the greater the saturation flow.



Sat. Flow (veh/hr/ln)		Opposing Traffic (veh/hr)				
		100	1,000	2,000	3,000	4,000
$S \times W/1,000$	0.5	1,377	593	225	82	29
	1.0	1,265	512	180	61	20
	1.5	1,168	445	146	46	14
	2.0	1,084	388	118	34	9
	2.5	1,011	340	96	26	6

**Figure 5.5– Saturation Flow Rate as a Function of Opposing Traffic and  $S \times W/1,000$**

Notes: S=posted speed limit; W=width of opposing lanes.

## 6 Conclusions

The saturation flow rate is an essential component of left turn capacity estimation at signalized intersections with a permissive left turn phase. Two gap acceptance parameters are the foundation for estimating the saturation flow: critical and follow-up headways. This study presents an evaluation of the effect of different factors on gap acceptance parameters and saturation flow of left turns at signalized intersections (NAS 2016).

Video data was collected at 27 intersections from five states in different geographical regions of the United States— Arizona, Florida, North Carolina, Virginia, and Wisconsin. Based on the geometric characteristics, coverage of video field of view, one or multiple left turn approaches at each intersection were used for analysis. Thus, a total of 45 approaches served to evaluate left turn gap acceptance of over 2,500 left-turning vehicles at signalized intersections.

Using the ML method proposed by Troutbeck (2014), mean critical headway estimates from all approaches ranged between 3.68 and 6.41 seconds. The aggregated mean critical headway was 4.87 seconds with a standard deviation of 1.54 seconds. The mean follow-up headway estimates for all approaches ranged between 2.03 and 4.36 seconds. The aggregated mean follow-up headway was 2.73 seconds with corresponding standard deviation of 0.97 seconds. Aggregated critical and follow-up headway estimates of this study were higher (statistically significant) than the HCM estimates. The mean critical headway for large vehicles was 6.03 seconds with a standard deviation of 1.37 seconds. Despite the limited number of observations, the mean critical headway for large vehicles is different than the aggregated estimate of 4.87 seconds which only included passenger vehicles.

Existing critical and follow-up headway estimates do not account for geometric and operational measures, so the saturation flow does not reflect intersection site-specific characteristics. In this study, meta-regression models were developed as a function of the posted speed limit and width of opposing traffic ( $S \times W/1,000$ ). Thus, the saturation flow can be directly evaluated as a function of these predictor variables and opposing traffic

flow. Results show that with a decreasing value of the posted speed limit and width of opposing traffic lanes, the smaller the critical and follow-up headways result in higher saturation flow estimates.

Driver distraction, green ball or flashing yellow arrow signal indication, pedestrians, and obstruction of line of sight were not addressed in this report, as there were not enough observations to conduct a detailed analysis. However, future research efforts should focus on addressing the influence of these other factors on gap acceptance behavior.

## References

- Alhajyaseen, W. K., Asano, M., & Nakamura, H. (2013). Left-turn gap acceptance models considering pedestrian movement characteristics. *Accident Analysis & Prevention, 50*, 175-185.
- Ashworth, R. (1968). A note on the selection of gap acceptance criteria for traffic simulation studies. *Transportation Research, 2*(2), 171-175.
- Borenstein, M., Hedges, L. V., Higgins, J. P., & Rothstein, H. R. (2021). *Introduction to meta-analysis*. John Wiley & Sons.
- Brilon, W. (1988). Recent developments in calculation methods for unsignalized intersections in West Germany. In *Intersections without traffic signals* (pp. 111-153). Springer, Berlin, Heidelberg.
- Brilon, W., Koenig, R., & Troutbeck, R. J. (1999). Useful estimation procedures for critical gaps. *Transportation Research Part A: Policy and Practice, 33*(3-4), 161-186.
- Cassidy, M. J., Madanat, S. M., Wang, M. H., & Yang, F. (1995). Unsignalized intersection capacity and level of service: revisiting critical gap. *Transportation research record, (1484)*, 16-23.
- Daily, C., Tantillo, M., Chun, P., Wilcox, N., Conran, C., Cynecki, M., ... & Rodriguez, B. C. (2019). *Decision-Making Guide for Traffic Signal Phasing* (No. NCHRP Project 03-118).
- Devarasetty, P. C., Zhang, Y., & Fitzpatrick, K. (2012). Differentiating between left-turn gap and lag acceptance at unsignalized intersections as a function of the site characteristics. *Journal of transportation engineering, 138*(5), 580-588.
- Drew, D. R. (1968). *Traffic flow theory and control* (No. 467 pp).

- Harders, J. (1968). Die Leistungsfähigkeit nicht signalgeregelter städtischer Verkehrsknotenpunkte. *Series Strassenbau and Strassenverkehrstechnik*, (76).
- Hewitt, R. H. (1983). Measuring critical gap. *Transportation science*, 17(1), 87-109.
- Hurwitz, D. S., Monsere, C., Tuss, H., Paulsen, K., & Marnell, P. (2013). *Improved pedestrian safety at signalized intersections operating the flashing yellow arrow* (No. OTREC-RR-13-02). Oregon Transportation Research and Education Consortium.
- Hutton, J. M., Bauer, K. M., Fees, C. A., & Smiley, A. (2015). Evaluation of left-turn lane offset using the naturalistic driving study data. *Journal of safety research*, 54, 5-e1.
- Joshua, S. C., & Saka, A. A. (1992). *Mitigation of sight-distance problem for unprotected left-turning traffic at intersections* (No. 1356).
- Knodler Jr, M. A., & Noyce, D. A. (2005). Tracking driver eye movements at permissive left-turns. In *Proceedings of the 3rd International Driving Symposium on Human Factors in Driver Assessment, Training, and Vehicle Design*, Rockport, ME.
- Knodler Jr, M. A., Noyce, D. A., & Fisher, D. L. (2007). Evaluating effect of two allowable permissive left-turn indications. *Transportation research record*, 2018(1), 53-62.
- Knodler Jr, M. A., Noyce, D. A., Kacir, K. C., & Brehmer, C. L. (2006). Analysis of driver and pedestrian comprehension of requirements for permissive left-turn applications. *Transportation research record*, 1982(1), 65-75.
- Messer, C. J., Fambro, D. B., & Andersen, D. A. (1975). *A Study of the Effects of Design and Operational Performance of Signal Systems--Final Report* (No. TTI-2-18-75-203-2F Final Rpt.).
- Miller, A. J. (1971). Nine estimators of gap-acceptance parameters. *Publication of: Traffic Flow and Transportation*.

- Noyce, D. A., Bergh, C. R., & Chapman, J. R. (2007). *Evaluation of the flashing yellow arrow permissive-only left-turn indication field implementation*. National Cooperative Highway Research Program, National Academy of Sciences.
- Ogallo, H. O., & Jha, M. K. (2014). Methodology for critical-gap analysis at intersections with unprotected opposing left-turn movements. *Journal of Transportation Engineering*, 140(9), 04014045.
- Raff, M. S. (1950). A volume warrant for urban stop signs. Eno Foundation for Highway Traffic Control. Saugatuck, Connecticut.
- Saka, A. A. (1998). Effect of dynamic sight-distance problem on unprotected left-turn movement capacity. *Journal of transportation engineering*, 124(3), 223-228.
- Siegloch, W. (1973). Die leistungsermittlung an knotenpunkten ohne lichtsignalsteuerung. *Series Strassenbau and Strassenverkehrstechnik*, (154).
- The National Academics of Sciences, Engineering, Medicine. (2016). *Highway Capacity Manual: A Guide for Multimodal Mobility Analysis*. Transportation Research Board.
- Tian, Z., Troutbeck, R., Kyte, M., Brilon, W., Vandehey, M. A. R. K., Kittelson, W., & Robinson, B. (2000, June). A further investigation on critical gap and follow-up time. In *Proceedings of the 4th International Symposium on Highway Capacity, Maui/Hawaii, Transportation Research Circular E-C018* (pp. 409-421).
- Troutbeck, R. J. (2014). Estimating the mean critical gap. *Transportation Research Record*, 2461(1), 76-84.
- Troutbeck, R. J., & Brilon, W. (2005). Unsignalized intersection theory, revised monograph on traffic flow theory. *FHWA, US Department of Transportation*.
- Viechtbauer, W. (2010). Conducting meta-analyses in R with the metafor package. *Journal of statistical software*, 36(3), 1-48.



Yan, X., & Radwan, E. (2008). Influence of restricted sight distances on permitted left-turn operation at signalized intersections. *Journal of transportation engineering*, 134(2), 68-76.

Zheng, D., Chitturi, M. V., Bill, A. R., & Noyce, D. A. (2012). Critical gaps and follow-up headways at congested roundabouts. In *Transportation Research Board Annual Meeting, Washington*.

Zohdy, I., Sadek, S., & Rakha, H. A. (2010). Empirical analysis of effects of wait time and rain intensity on driver left-turn gap acceptance behavior. *Transportation research record*, 2173(1), 1-10.